Proceedings World Geothermal Congress 2026
Calgary, Canada, June 8 – 11, 2026

Modelling Thermal Response and Tracer Tests in a Complex Fractured Aquifer System

Meissam L. Bahlali[1]*, Carl Jacquemyn[1], Matthew Jackson[1], Adrian Butler[2], Joseph Kelly[3], Fleur Loveridge[3], Dave Boon[4], Jason Ngui[4], Ed Hough[4], Oliver Kuras[4], Jonathan Chambers[4], Katerina Kyrkou[5] and Adam Booth[5]

Department of Earth Science and Engineering, Imperial College London[1]*, Department of Civil and Environmental Engineering, Imperial College London[2], School of Civil Engineering, University of Leeds[3], British Geological Survey[4], School of Earth and Environment, University of Leeds[5]

m.bahlali@imperial.ac.uk

Keywords: Chalk aquifer, numerical modelling, open-loop thermal tracer test (OL-TTT), aquifer heterogeneity, heat transport

INTRODUCTION

The Chalk aquifer is an important groundwater resource in the UK and supports over 50 open-loop geothermal systems. However, its complex hydrogeology makes it difficult to predict thermal plume behaviour and the efficient operation of geothermal installations. The Chalk aquifer exhibits a dual-porosity structure, characterised by high-permeability fractures embedded within a low-permeability matrix. This heterogeneity leads to highly variable groundwater velocities under both natural and pumped conditions (Butler et al., 2009; Jackson et al., 2012). This work presents numerical modelling of an open-loop thermal tracer test (OL-TTT) conducted at Trumpletts Farm, a well-instrumented experimental site in Berkshire, UK (Fig. 1a). The site includes six boreholes, each extending approximately 100 m into the Chalk, and is located near a large-capacity abstraction well used for river level management (Fig. 1b). A thermal response test (TRT) was previously conducted at the site (Loveridge et al., 2025b) and the results informed the models developed here. Following this TRT, an OL-TTT is planned for the site. The OL-TTT will be extensively instrumented for monitoring, including distributed temperature sensors in both the tested and offset boreholes, surface and cross-well electrical resistivity tomography and seismic monitoring (Loveridge et al., 2025a). The OL-TTT is designed to investigate heat transport processes, track thermal plume evolution, and assess the potential for thermal interference. This study focuses on addressing several key questions:

- Duration of monitoring: How long should temperature changes be monitored?
- Plume travel distance: How far will the thermal plume migrate within the aquifer?
- Thermal perturbation in time: How long will the temperature anomaly persist in the system?

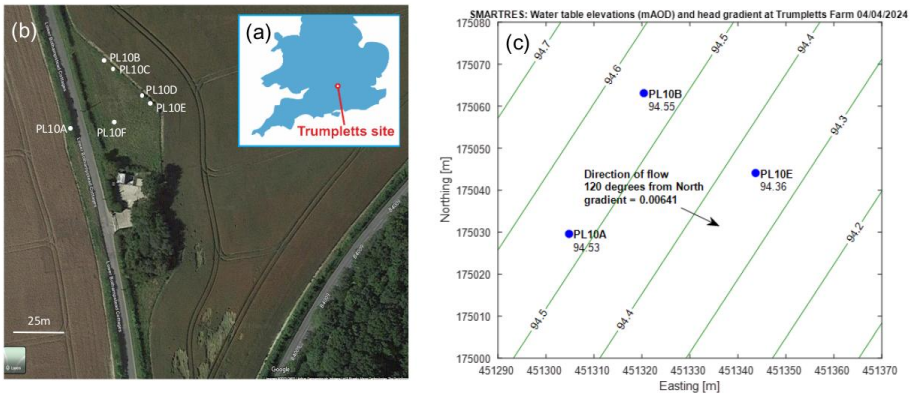


Figure 1. Overview of the Trumpletts field experimental site showing (a) location in the UK, (b) layout of boreholes and (c) measured water depth at the time of the TRT test with interpreted groundwater flow direction and head gradient.

1 OPEN LOOP THERMAL TRACER TEST

The OL-TTT will be performed using borehole PL10B for injection, with abstraction from PL10E (Fig. 1b). The flow induced by the test is generally aligned with the site's natural groundwater flow (Fig. 1c). The experimental setup includes:

- Distributed Temperature Sensing (DTS): fibre-optic cables installed in boreholes for high-resolution temperature monitoring.
- Cross-well Electrical Resistivity Tomography (ERT), used to visualise subsurface temperature variations.
- Seismic monitoring, to provide additional information on fracture connectivity.
- Injection and abstraction: Groundwater will be abstracted from PL10E at a rate of 2.5 L/s, heated to 20.7°C, and injected into PL10B at the same rate, with simultaneous downstream abstraction at PL10E.

2 NUMERICAL MODELLING

The open-source IC-FERST code (https://multifluids.github.io/; see Regnier et al., 2022; Salinas et al., 2021) was used to simulate fluid flow and heat transport. Figure 2 presents a schematic of the numerical model setup. The model was based on a geological framework derived from previous pumping tests (Jackson et al., 2012) and the earlier TRT (Loveridge et al., 2025b). High-permeability zones were explicitly included to account for observed groundwater cross-flow, upflow, and heat transport away from the borehole during the TRT. A series of simulations was performed to assess the influence of hydraulic properties and heat transfer assumptions on thermal plume evolution. Eight scenarios were considered:

- Scenario 1: High-permeability zone 1 = 1.7×10^{-11} m^2, dispersivity = 1 m, thermal equilibrium.
- Scenario 2: High-permeability zone 1 = 1.7×10^{-11} m^2, dispersivity = 10 m, thermal equilibrium.
- Scenario 3: High-permeability zone 1 = 5×10^{-11} m^2, dispersivity = 1 m, thermal equilibrium.
- Scenario 4: High-permeability zone 1 = 5×10^{-11} m^2, dispersivity = 10 m, thermal equilibrium.
- Scenario 5: High-permeability zone 1 = 1.7×10^{-11} m^2, dispersivity = 1 m, non-thermal equilibrium.
- Scenario 6: High-permeability zone 1 = 1.7×10^{-11} m^2, dispersivity = 10 m, non-thermal equilibrium.
- Scenario 7: High-permeability zone 1 = 5×10^{-11} m^2, dispersivity = 1 m, non-thermal equilibrium.
- Scenario 8: High-permeability zone 1 = 5×10^{-11} m^2, dispersivity = 10 m, non-thermal equilibrium.

Thermal non-equilibrium models are particularly relevant for fractured aquifers, where heat is mainly transported along fractures while the surrounding matrix acts as a heat reservoir. In contrast, thermal equilibrium models assume instantaneous heat exchange between fractures and matrix, meaning heat exchange between them is highly efficient. However, heat transfer between fractures and the matrix may be limited due to the short residence time of water in fractures. Non-equilibrium scenarios therefore provide a more realistic representation of fracture-dominated flow, where heat is transported rapidly along preferential fracture flow paths with minimal exchange with the rock matrix. Additionally, sensitivity analyses were conducted by varying the groundwater flow direction by ±30° to evaluate how changes in natural flow direction influence plume evolution. The initial aquifer temperature was 10.7°C, determined from borehole logging. The injection was designed at a rate of 2.5 L/s for six days. Boundary conditions were set using pressure and temperature data from earlier hydrological investigations (Jackson et al., 2012). Fracture zone permeability was calibrated against observed pressure responses during past pumping at PL10B. Two calibration outcomes emerged: one set of simulations reproduced drawdown at PL10A and PL10B (corresponding to scenarios 1, 2, 5, and 6), while another matched drawdown at PL10D and PL10E (scenarios 3, 4, 7, and 8). No attempt was made at this stage to reconcile both sets of observations simultaneously.

Aquifer properties were specified under water-saturated conditions. The Chalk matrix was represented with a total porosity of 0.4, effective porosity of 0.01, and permeability of 9.87×10^{-15} m^2. Thermal properties were set as a density of 1869 kg/m^3, heat capacity of 1550 J/kg.K, and thermal conductivity of 2.55 W/m.K (wet values; from the British Geological Survey, Bloomfield et al., 1995 and Law, 2010). A shallow vadose zone was assigned a permeability of 9.87×10^{-16} m^2. High-permeability fracture zones were parameterized separately. The shallowest zone (High-perm zone 1 in Fig. 2) was assigned either 1.7×10^{-11} m^2 (scenarios 1, 2, 5, and 6) or 5×10^{-11} m^2 (scenarios 3, 4, 7, and 8), while the deeper high-permeability zones were fixed at 1.7×10^{-11} m^2 in all cases.

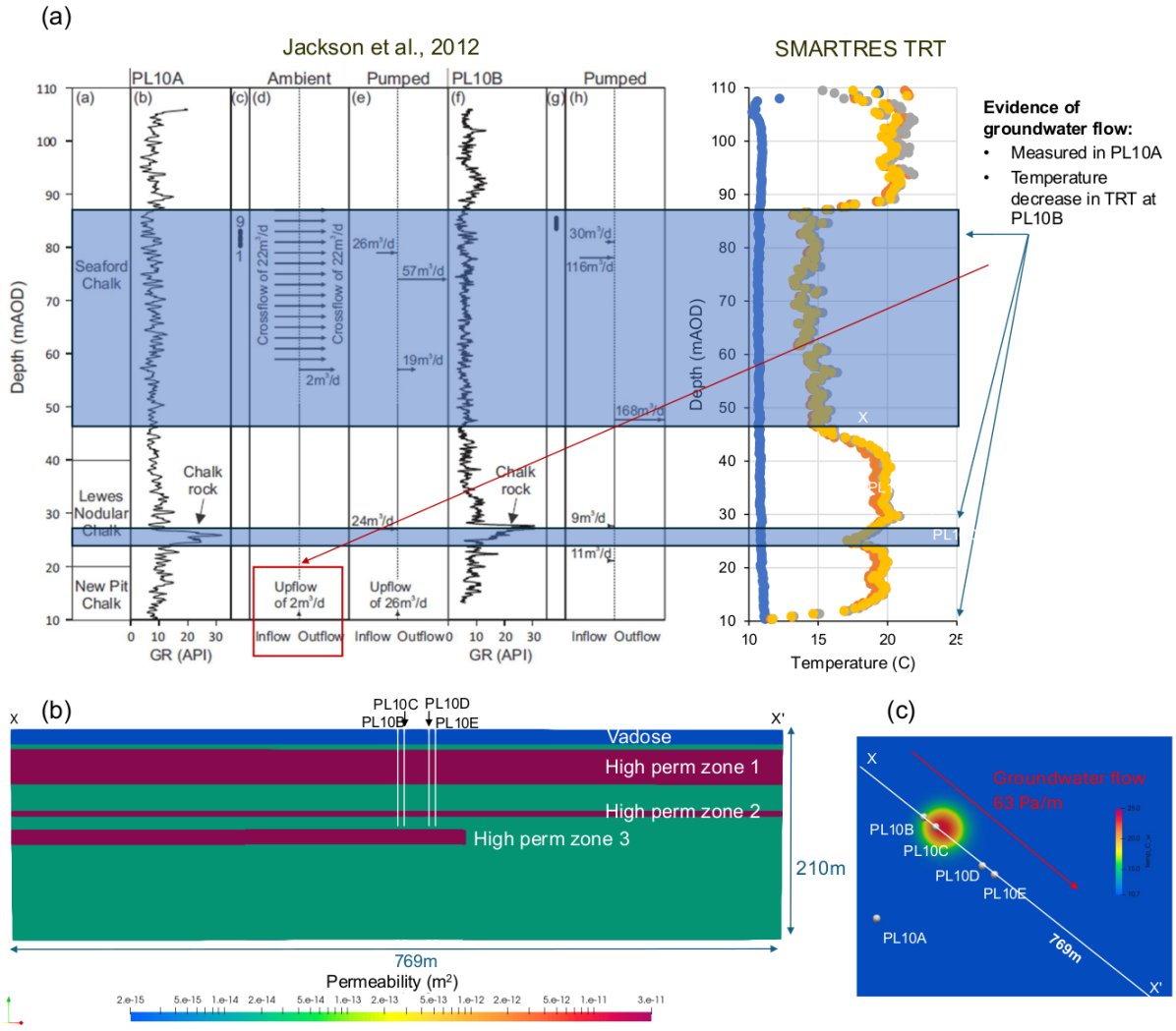


Figure 2. Data from boreholes PL10A and PL10B. (a) shows gamma ray logs and interpreted groundwater flow and ambient conditions and during pumping from the abstraction well (after Jackson et al. 2012), and temperature measured as a function of depth along PL10B during the TRT (from Loveridge et al., 2025b). The blue zones indicate interpreted high permeability layers, thought to represent highly fractured intervals. (b) is a cross-section X-X' through the 3D numerical model, showing the corresponding high permeability layers. (c) is a top view of the model, showing a snapshot of the simulated thermal plume in one of the simulation cases.

3 RESULTS AND DISCUSSION

Figure 3 shows the time required to reach the maximum temperature at each well (Fig. 3a) and the associated temperature difference (Fig. 3b). Clear differences emerge between scenarios. In the high-dispersivity cases (scenarios 2 and 4), heat transport is more diffuse, with the plume extending further along the flow direction but at lower peak temperatures. The spreading effect leads to a less concentrated thermal front. As a result, while the plume reaches neighbouring wells more quickly, the temperature at those wells is lower, as the thermal energy has been dispersed over a larger volume of water. In scenarios 3 and 4, which assume higher fracture-zone permeability, the plume migrates faster than in scenarios 1 and 2. Enhanced permeability accelerates groundwater flow, which then allows the thermal plume to reach neighbouring wells sooner. The impact of these contrasting behaviours is reflected in the predicted temperatures at PL10C and PL10E. In scenario 1 (low dispersivity, equilibrium), the maximum peak temperature at PL10C reached 15.6°C after 26 days, while at PL10E the peak was 11.6°C after 210 days. By contrast, in scenario 6 (high dispersivity, non equilibrium), the peak temperature at PL10C was much lower at 10.71°C after 7 days, and at PL10E it was 10.75°C after 95 days, which is less than 0.1 °C above the ambient temperature of 10.7°C. These differences are explained by both dispersivity and heat transfer conditions. Under high dispersivity, heat spreads further along the flow direction, causing the thermal plume to be more diffused. This diffusion reduces the peak temperature at each location, making it less likely to produce measurable temperature changes in the surrounding wells. The thermal front is

less concentrated and spreads out over a larger area, so although it reaches neighbouring wells faster, the temperature at those wells is lower than in the low-dispersivity case. The contrast between equilibrium and non-equilibrium conditions is even greater. In thermal equilibrium cases, heat is transferred efficiently between groundwater and the rock matrix. That leads to higher peak temperatures. Under non-equilibrium conditions, where heat exchange between fractures and matrix is limited, temperature increases are smaller and slower. For example, as seen earlier, the maximum rise under non-equilibrium conditions was less than 0.1°C above ambient at all the wells. These results have direct implications for monitoring. At PL10C, a peak of 15.6°C after 26 days in the low-dispersivity equilibrium case represents a strong signal that would likely be detectable using geophysics. At PL10E, however, the maximum of 11.6°C occurs only after 210 days, making detection less practical in the short term. Monitoring at PL10E therefore only appears viable over long timescales, and even then, detectability will depend strongly on the sensitivity of the methods employed. In the high-dispersivity non-equilibrium cases, temperature changes are minimal and are unlikely to be detected.

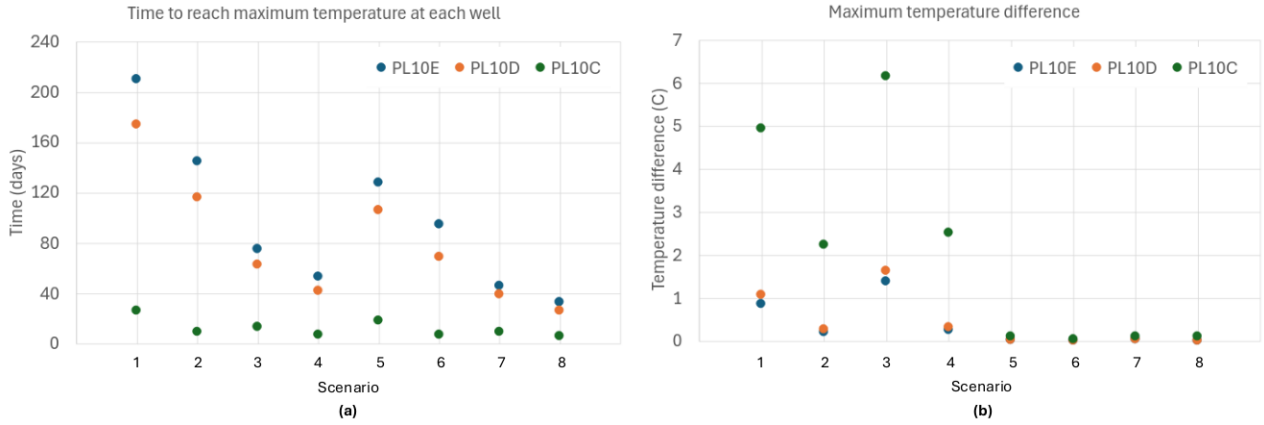


Figure 3. Summary of heat transport behaviour under different scenarios. (a) Time to reach the maximum temperature at each well. (b) Corresponding temperature difference.

CONCLUSIONS

Numerical simulations of the proposed open-loop thermal tracer test (OL-TTT) in a fractured Chalk aquifer highlight the dominant influence of fracture networks on thermal transport. Key findings include:

- High dispersivity produces broader thermal plumes but with lower peak temperatures.
- Assuming local thermal equilibrium can underestimate plume migration distances.
- Surface geophysical monitoring may have limited effectiveness in detecting temperature changes due to the small thermal anomalies in the aquifer.
- A major challenge for OL-TTT in fractured aquifers with high groundwater flow is delivering sufficient heat to generate a detectable plume.

Future work will focus on ongoing numerical simulations of a closed-loop thermal response test (TRT) at the same site, which will further inform the design and optimisation of geothermal systems in fractured aquifers.

Acknowledgements

This work is part of the SmartRes project ("Smart Assessment, management and optimisation of urban geothermal resources") (see https://www.imperial.ac.uk/earth-science/research/research-projects/smartres/). The project is funded by the UK Natural Environment Research Council (NERC) under grant NE/X005496/1.

REFERENCES

Butler, A.P., Mathias, S.A., Gallagher, A.J., Peach, D.W., Williams, A.T.: Analysis of flow processes in fractured chalk under pumped and ambient conditions (UK), *Hydrogeology Journal*, **17(8)**, (2009), pp.1849-1858.

Jackson, M.D., Butler, A.P. and Vinogradov, J.: Measurements of spontaneous potential in chalk with application to aquifer characterization in the southern UK, *Geological Society of London* (2012).

Jackson, M.D., Regnier, G. and Staffell, I.: Aquifer Thermal Aquifer Thermal Energy Storage for low carbon heating and cooling in the United Kingdom: Current status and future prospects, *Applied Energy* **376** (2024), 124096. https://doi.org/10.1016/j.apenergy.2024.124096.

Loveridge, F., Boon, D., Al-Jawad, J., Hough, E., Parker, K., Butler, A., Bahlali, M., Jackson, M., Ngui, J., Kyrkou, K., Kelly, J., Booth, A., Thompson, J.: Open loop thermal tracer tests to characterise fracture aquifers for shallow geothermal applications, *Proceedings*, European Geothermal Congress 2025, Zurich, Switzerland (2025).

Loveridge, F., Kyrkou, K., Kelly, J., Ngui, Y., Booth, A., Chambers, J., White, A., Boon, D., Kuras, O., Hough, E.: Enhanced in situ thermal response testing with distributed thermal sensing and electrical resistivity tomography, *Proceedings*, European Geothermal Congress 2025, Zurich, Switzerland (2025).

Law, R.: Geothermal systems in the Chalk of the south east of England: methods of predicting thermal transport in a fractured aquifer (Doctoral dissertation, University of Birmingham, 2010).

Regnier G., Salinas P., Jacquemyn C. and Jackson M.D.: Numerical simulation of aquifer thermal energy storage using surface-based geologic modelling and dynamic mesh optimisation, *Hydrogeology Journal,* **30**, (2022), 1179–98. http://dx.doi.org/10.1007/s10040-022-02481-w.

Salinas, P., Regnier, G., Jacquemyn, C., Pain C.C. and Jackson, M.D., Dynamic mesh optimisation for geothermal reservoir modelling, *Geothermics*, **94**, (2022), 10289. https://doi.org/10.1016/j.geothermics.2021.102089.